Environmental Science Advances

ROYAL SOCIETY OF CHEMISTRY

PAPER

View Article Online
View Journal | View Issue

Cite this: *Environ. Sci.: Adv.*, 2022, **1**, 470

Gaseous emissions of a heavy-duty engine fueled with polyoxymethylene dimethyl ethers (OME) in transient cold-start operation and methods for after-treatment system heating†

Alexander D. Gelner, *[a] Genny A. Pang, [ac] Markus Weber, [a] Christoph Haisch, [a] Harald A. Beck,[b] Christian Pastoetter,[b] Martin Härtl, [a] Malte Jaensch [a] and Georg Wachtmeister[a]

Polyoxymethylene dimethyl ethers (OME) are promising e-fuels for diesel engines, combining carbon-neutral production and low-emission engine operation by virtue of soot-free combustion. The emissions of diesel engines fueled with OME and in blends with diesel have been studied extensively using single-cylinder research engines under laboratory conditions. Emissions from a series engine using an exhaust after-treatment system (ATS) – especially in cold-start operation – are largely unexplored. This study presents investigations conducted using a heavy-duty engine with ATS in a transient driving cycle including cold-start operation. Measurements from a Fourier transform infrared spectrometer (FT-IR) showed that formaldehyde and formic acid form the largest proportion of the monitored tailpipe exhaust emissions due to incomplete combustion in cold-start operation, as long as the catalysts are below their light-off temperature. Non-target screening using a mass spectrometer for online characterization of both gaseous and aerosol exhaust revealed that unburned OME accounts for the majority of gaseous emissions of heavy species in raw exhaust, independent of cold- or hot-start. The ATS removes OME in the exhaust equally in the cold and the hot run. Additionally, this study presents results with specific measures taken for ATS heating such as electrical heating and fuel dosing – demonstrating that electrical heating in combination with an early start of fuel dosing reduces nitrogen oxide (NO_x) emissions in the transient driving cycle by 64.9%, but at the cost of an increase in formaldehyde emission of 58.3%. A later start of fuel dosing avoids this increase and reduces NO_x emissions by 61.8%.

Received 27th April 2022
Accepted 16th June 2022

DOI: 10.1039/d2va00080f

rsc.li/esadvances

Environmental significance

OME is a sustainable e-fuel which burns soot-free and therefore helps to reduce the impact of diesel engines on the environment regarding climate change and air pollution due to black carbon emission. However, incomplete combustion of OME results in the formation of other pollutants such as formaldehyde. In order to avoid the emission of these species and the emission of nitrogen oxides, exhaust after-treatment is necessary but requires operation above the light-off temperature of the catalysts. This study contains investigations on gaseous emissions of a heavy-duty engine fueled with OME with a state-of-the-art after-treatment system in transient cold-start and hot operation. A conventional exhaust analysis system and a novel approach for non-target screening in order to observe secondary emissions besides the well-known products of incomplete OME combustion is used. Additionally, the study evaluates two methods for after-treatment system heating in order to reduce the period of inactive catalysts and therefore to minimize environmental impact of an OME engine.

Introduction

It is widely accepted that greenhouse gas emissions from fossil fuel combustion are considered a significant cause of anthropogenic climate change, which is a central challenge of the 21st century.[1] Therefore, substituting fossil fuels with energy from renewable sources like wind or solar power is considered an essential solution to avoiding greenhouse gas emissions.[2] Storage of these renewable energies *via* the electricity-based synthesis of so-called "e-fuels" enables the potential for

[a]*Technical University of Munich (TUM), Schragenhofstraße 31, Munich 80992, Germany. E-mail: gelner@tum.de*

[b]*MAN Truck & Bus SE, Vogelweiherstraße 33, Nuremberg 90441, Germany*

[c]*Universität der Bundeswehr München, Werner-Heisenberg-Weg 39, Neubiberg 85577, Germany*

† Electronic supplementary information (ESI) available. See https://doi.org/10.1039/d2va00080f

climate-neutral operation of existing and future internal combustion engines.[3] In addition to synthetic e-fuels having similar properties to their fossil fuel counterpart, some so-called "tailored fuels" offer advantages such as lower pollutant combustion. For example, oxygenated fuels burn with significant lower soot and particle emissions.[4] In the case of diesel engines, oligomers from the series of polyoxymethylene dimethyl ethers (OME) are among the most promising alternatives.[5] The synthesis process for producing OME is based on hydrogen – which can be produced by means of electrolysis from renewable energies – and carbon dioxide, which comes from either direct air capture, post combustion capture, or point sources.[6] The combustion of OME is soot-free[4,7–10] by virtue of the lack of intramolecular C–C bonds.[11] In addition to the harmful effect of soot on human health,[12] black carbon is also regarded as an accelerator of climate change.[13] Soot-free combustion resolves the trade-off between soot and NO_x that is typical of fossil diesel and paraffinic alternatives,[7,14,15] thus enabling the reduction of NO_x emissions through in-engine measures without increasing the level of particulate emissions by soot formation.[14,16] NO_x emissions are considered harmful to the respiratory tract[17] and are initiators of photochemical smog.[18] In combination with a state-of-the-art exhaust after-treatment system (ATS), OME-fueled engines offer the possibility of ultra-low pollutant emissions, which was demonstrated in a previous study by Gelner *et al.* on a heavy-duty engine in a stationary and transient test cycle.[19] As with conventional diesel operation, however, effectiveness of the ATS requires a system that is hot from engine operation. Due to successive adjustments to exhaust gas legislation, emissions in the so-called cold start – *i.e.* before the light-off temperature of the catalytic converters is reached – play an increasingly important role in passing emission tests.[20] Williams *et al.* demonstrated that most of the NO_x emissions were emitted during the first minutes of a driving cycle during cold-start operation.[21] Here both the oxidation of gaseous products of incomplete combustion, such as carbon monoxide or hydrocarbons by the diesel oxidation catalyst (DOC), and the reduction of NO_x by selective catalytic reduction (SCR) are inhibited. Whereas cold-start emissions from fossil or biodiesel have been studied in sufficient detail,[22–26] cold start emissions from OME operations remain uninvestigated. Härtl *et al.*,[4] Barro *et al.*[27] and Pélerin *et al.*[14] demonstrated formaldehyde (CH_2O) and methane (CH_4) emissions during incomplete OME combustion on a preconditioned single-cylinder research engine, which is why these emissions can also be assumed to occur during cold starts. Moreover, the results by Zengel *et al.*[28] and Elsener *et al.*[29] showed the formation of hydrogen cyanide (HCN) in the SCR system under the presence of CH_2O and NH_3. The results of Gelner *et al.* did not show any tailpipe emission of HCN with a hot ATS.[19] They assumed a combination of oxidative catalysts upstream and downstream of the SCR stage to be essential for avoiding the tailpipe emission of HCN because of the prior oxidation of CH_2O and the downstream oxidation of eventually formed HCN.

To keep the period of an inactive ATS as short as possible, various methods have been established to speed up heating of the ATS, which have been discussed by Gao *et al.* along with a discussion of their effectiveness.[30] Additionally, fuel dosing, in which the supply of unburned fuel to the DOC for catalytic combustion heats the downstream components of the ATS using the heat released from the exothermic reaction, is another effective method for reducing the period of inactive ATS.[31] Fuel dosing is restricted in diesel operation by a phenomenon known as face plugging. The resulting hydrocarbon (HC) emissions in combination with soot particles block the active centers of the DOC, and thus lead to inactivation of the catalytic surface.[32] Gelner *et al.* demonstrated the effectiveness of fuel dosing on a heavy-duty engine in OME operation using a DOC, but limited by a CH_2O slip.[31] In contrast to diesel operation, however, this slip is indirectly proportional to the injection quantity. Therefore, fuel dosing was considered to be a promising method for reducing the inactive ATS period due to soot-free combustion – and thus avoidance of face plugging – as long as the remaining ATS components are removing CH_2O slip.

This study investigates the gaseous emissions occurring in the homologation-relevant World Harmonized Transient Cycle (WHTC) driving cycle in an OME-fueled heavy-duty engine equipped with an ATS. The cold and hot cycles are compared in order to distinguish between cold-start-induced emissions and emissions that also occur at operating temperature. A custom-built mass spectrometer (MS) system was employed for supplementary non-target screening of gaseous emissions in order to identify any possible unknown substances in the exhaust which were not accounted for in the primary Fourier transform infrared spectrometer (FT-IR) concentration measurements of the exhaust. In addition, the MS employed was calibrated for quantitative OME concentration measurement at a higher sensitivity than the FT-IR used. Moreover, electrical heating of the DOC according to Maus *et al.*[33] was employed in combination with the fuel dosing suggested by Gelner *et al.*[31] The operating strategy was varied so as to enable evaluation of the effectiveness of various methods for reducing the length of the cold-start period.

Materials and methods

Fuel

OME are oligomers with different chain lengths and have the general structure of $CH_3–O–(CH_2O)_n–CH_3$, where n is the number of inner-molecular oxymethylene groups. The abbreviation OME_n indicates the respective chain length of the molecule. In this study, the fuel mixture used for the experiments contained several OME_n with major percentages of $n = 3$–6 (OME_3: 58%, OME_4: 29%, OME_5: 10%, OME_6: 2%). The proportion of shorter- or longer-chain OME was less than 1%. As additives, the fuel also contained 300 mg kg^{-1} each of butylated hydroxytoluene (BHT) as an antioxidant as well as a flow improver. This mixture will be simply abbreviated as OME in the remainder of this paper. ASG Analytik-Service AG (Germany) provided the OME fuel used and measured the property values. Table 1 in the ESI† contains these values and the respective standard of the measurement method used. The mixture fulfills the M DIN TS 51699 standard for OME fuel.[34] As

a reference, "diesel" describes fossil fuel according to the EN 590 standard[35] having a maximum content of 7% (v/v) fatty acid methyl esters (FAME). Table 1 presents the physico-chemical properties of the OME fuel mixture and presents a comparison of the properties with fossil diesel. The diesel values are largely from the fuel EN 590 standard. When the standard did not provide information about a specific property, this value was taken from Lautenschütz *et al.*[36] The oxygen content calculation was based on the assumption that the FAME content consists of oleic acid, with the respective values coming from Hoekman *et al.*[37]

Given an oxygen content of 45% (w/w), the OME mixture used had a reduced lower heating value (LHV) than fossil diesel. The higher OME density partially compensates this to a volumetric diesel equivalent ratio of

$$\frac{\mathrm{LHV_{diesel}}}{\mathrm{LHV_{OME}}} \cdot \frac{\rho_{\mathrm{diesel}}}{\rho_{\mathrm{OME}}} \approx 1.75 \quad (1)$$

The cetane number of OME exceeds the requirements of the EN 590 standard. The higher cetane number indicates excellent ignitability, which enables engine operation without pilot injection, as demonstrated in previous studies.[14,38] The boiling range of OME is similar to that of diesel, but with an initial start and end of boiling at lower temperatures. The flash point of OME surpasses the EN 590 value. The boiling range and flash point enable OME storage and distribution similar to that of fossil diesel. The lubricity of OME exceeds the requirement of the standard, while the kinematic viscosity is below the specification interval of the EN 590 standard. The sulfur content of OME is lower than 5 ppm, so it achieves the lower limit of the sulfur content determination standard. Furthermore, the OME mixture used contained an amount of 233 mg kg^{-1} CH_2O, which is a reactant in the synthesis process of OME.[39] The additive BHT prevents the decomposition of OME and therefore inhibits an increase in the CH_2O concentration in the fuel.[40]

Test engine

This study employed a MAN D2676LF51 heavy-duty six-cylinder diesel engine with two modifications besides the OME-adapted application of the electronic control unit of the state-of-the-art diesel operation:[1] the high-pressure pump was equipped with adapted seals which prevent swelling of the sealing material due to the different chemical polarity of OME,[2] the injectors in OME operation differed in nozzle geometry in order to compensate for the reduced LHV by a higher nozzle flow rate. The second modification prevented the need for higher injection durations on high-load points, which would have resulted in an increase in combustion duration and therefore in a reduction in efficiency.[41] Longer injection durations could also lead to interactions of the fuel jet with the lubricating film during the downward movement of the piston since the liner would be revealed. Moreover, the increase in nozzle flow rate enabled a reduction of rail pressure at low- and medium-load points – an important lever for decreasing NO_x emissions.[14,15] Table 2 illustrates the properties of the test engine used. The engine application was the same as in the previous study,[19] with a focus on a higher dynamic of the exhaust gas recirculation (EGR) valve.

After-treatment system and test bench setup

A modular twin-dosing system with an electrically heatable diesel oxidation catalyst (e-DOC), provided by VT Vitesco Technologies Emitec GmbH (Germany), was used for the ATS in this study. The catalysts were connected *via* flanges and pipes. Table 3 shows the properties of the ATS components in sequential downstream order. The e-DOC contained a separate heating disc in front of the platinum (Pt)-palladium (Pd)-coated structure of the DOC monolith. The heating disc had the same coating as the monolith. Two commercial heavy-duty vehicle batteries connected in series at 12 V and 220 Ah each supplied the e-DOC with electrical power. The resulting battery voltage of 24 V and the ohmic resistance of approximately 0.08 Ω resulted in an electrical current of about 300 A. The electrical power of the e-DOC was thus about 7.2 kW. A custom-built controller provided by VT Vitesco Technologies GmbH enabled the heating disc power supply to switch on and off. The designation of "twin dosing design" is derived from the structure of the ATS, which has components for NO_x reduction by means of SCR at

Table 1 Physico-chemical properties of the OME fuel mixture and fossil diesel. The values of diesel are from the standard EN 590[35] except from the LHV and boiling range, which are from Lautenschütz *et al.*[36] and the oxygen content, with the calculation using values from Hoekman *et al.*[37] This calculation assumes the FAME content to consist of oleic acid. ASG Analytik-Service AG measured the values for OME

	Diesel	OME
Oxygen content in % (w/w)	0–1[37] (with max. 7% (v/v) FAME)	45
Lower heating value in MJ kg^{-1}	42.6[36]	19.2
Density in kg m^{-3} at 15 °C	820–845	1057
Volumetric diesel equivalent ratio	1	1.75
Cetane number	>51	69
Boiling range in °C	170–390[36]	145–242
Kinematic viscosity in mm^2 s^{-1} at 40 °C	2.0–4.5	1.082
Lubricity – HFRR at 60 °C in μm	≤460	320
Flash point in °C	>55	65
Sulfur content in ppm	<10	<5
Formaldehyde content in mg kg^{-1}	—	233

Table 2 Properties of the test engine MAN D2676LF51. The injectors in OME operation have a higher nozzle flow rate to reduce the combustion duration at high-load points

Number of cylinders	6 (inline)
Bore	126 mm
Stroke	166 mm
Displacement	12419 cm^3
Compression ratio	18 : 1
Power	294 kW
Number of valves per cylinder	4 (2 inlet/2 exhaust)
Charge	Two-stage waste-gate turbocharger
Exhaust gas recirculation (EGR)	High-pressure & cooled
Injection system	Common rail (max. 1800 bar)
Hydraulic nozzle flow rate	Diesel: 1300 cm^3/30 s (at 100 bar)
	OME: 1835 cm^3/30 s (at 100 bar)

two different positions. In these subsystems, a doser injects aqueous urea solution as a reducing agent for the SCR reaction.

An EMITEC "GEN V" urea dosing pump provided delivery pressure for both dosers simultaneously. The urea dosage took place in an EMITEC "Universal Decomposition Pipe" (UDP) equipped with an EMITEC "JC-2" urea doser and a titanium dioxide (TiO_2) coated hydrolysis catalyst (Hyd), on which the conversion of urea to ammonia (NH_3) took place.[42] A downstream copper-zeolite (CuZe) SCR catalyst reduced NO_x *via* the reducing agent NH_3.[43] This catalyst was divided into three monolithic discs, thus enabling a modular catalyst volume increase or decrease. In the case of excess NH_3, the ammonia slip catalyst (ASC) oxidized this species selectively, thus avoiding the unselective oxidation of NH_3 to nitrous oxide (N_2O) in the downstream DOC,[44] which is desirable since N_2O is known to be a greenhouse gas with an enormous impact on climate change.[1] This DOC contained no heating disc. The downstream diesel particulate filter (DPF) was an uncoated Cordierite wall-flow filter. The second SCR system differed from the first in two major ways. First, the UDP in the second system was followed by a mixer for homogenization of the ammonia in the exhaust,[45] which was necessary given the usage of a different urea doser – an EMITEC "A^2-8" with varying spray targeting. The exhaust temperature was lower at the second SCR stage, which resulted in decreased decomposition of the injected urea.[45] Second, the second SCR catalyst had a larger volume than the one in the first stage, since it contained four monolithic discs instead of three. Moreover, the carrier structure differed slightly from that in the first system. Ideally, the second stage converts the remaining NO_x emissions. In contrast to the first SCR stage, the second stage had no ASC installed. The differences in the design of the two SCR stages resulted from the application to achieve the ultra-low NO_x emissions demonstrated in the previous study.[19]

Urea dosing was active in both SCR stages during the test cycles and considered the same starting temperatures as in standard diesel operation. The dosing strategy was based on ideal distribution between both stages in consideration of the temperature, the ammonia storage capacity, and the determined NO_x concentrations in the exhaust, which was similar to the experiments in the previous study.[19]

Fig. 1 shows a test bench setup scheme. The filtered air from the test bench air supply passes through an ABB MDM DN150 thermal dispersion mass flowmeter. This device determines the volumetric airflow for the calculation of the exhaust mass flow and the space velocity inside the catalysts, respectively. Downstream, another filter avoids contamination of the turbocharger compressor wheel. A two-stage turbocharger system with two intercoolers increases the boost pressure. The six-cylinder engine was equipped with an EGR valve, which controlled high-pressure EGR with intercooling. Two Type K thermocouples, each downstream of the hydrolysis catalysts, enabled monitoring of the exhaust temperature upstream of the respective SCR catalysts. Another thermocouple was installed upstream of the second DOC.

An IAG Versa FAS-05 FT-IR was set up for determining the concentration of the specific chemical species detected in emissions of the above-mentioned previous studies.[4,14,27] The chemical species include CH_4 and CH_2O. Additionally, the FT-IR was configured to measure methanol (CH_3OH), formic acid (CH_2O_2), HCN and several OME_n: dimethyl ether (DME or OME_0), dimethoxymethane (OME_1), and OME with a chain length of $n =$

Table 3 Properties of the ATS components provided by VT Vitesco Technologies Emitec GmbH in downstream order. The value of the Platinum Group Metals (PGM) density refers to the total quantity of the precious metal content. (*) The value of the open frontal area (OFA) is based on the following assumptions: coating of the DOC is 150 g dm^{-3}, coating of the UDP is 60 g dm^{-3} and coating of the SCR is 200 g dm^{-3}, the wash-coat density is 1.35 g cm^{-3} (**) Before the experiments of this study, the DPF had a mileage of about 500 km in diesel operation, but was regenerated in an oven at 500 °C for six hours

Component	Catalytic coating	PGM in g ft^{-3}	cpsi	Diameter in mm	Length in mm	Volume in dm^3	Carrier material	Carrier structure	OFA(*)
e-DOC	Pt, Pd (1 : 1)	35	N/A	285.8	101.5	6.51	Metal	300/600LS	82%
Hyd	TiO_2	—	N/A	174.6	60	1.43	Metal	300/600 LSPE	89%
SCR	CuZe	—	N/A	300	3 × 101.5	21.5	Metal	600 CS	79%
ASC	Pt	3	300	300	90	6.4	Metal	E300	78%
DOC	Pt, Pd (1 : 1)	35	300	300	150	10.6	Metal	300/600 LS	82%
DPF (**)	Uncoated	—	300	305	381	27.8	Cordierite	Symmetrical	83%
Hyd	TiO_2	—	N/A	174.6	60	1.43	Metal	300 PE	89%
SCR	CuZe	—	400	300	4 × 101.5	28.8	Metal	E400	77%

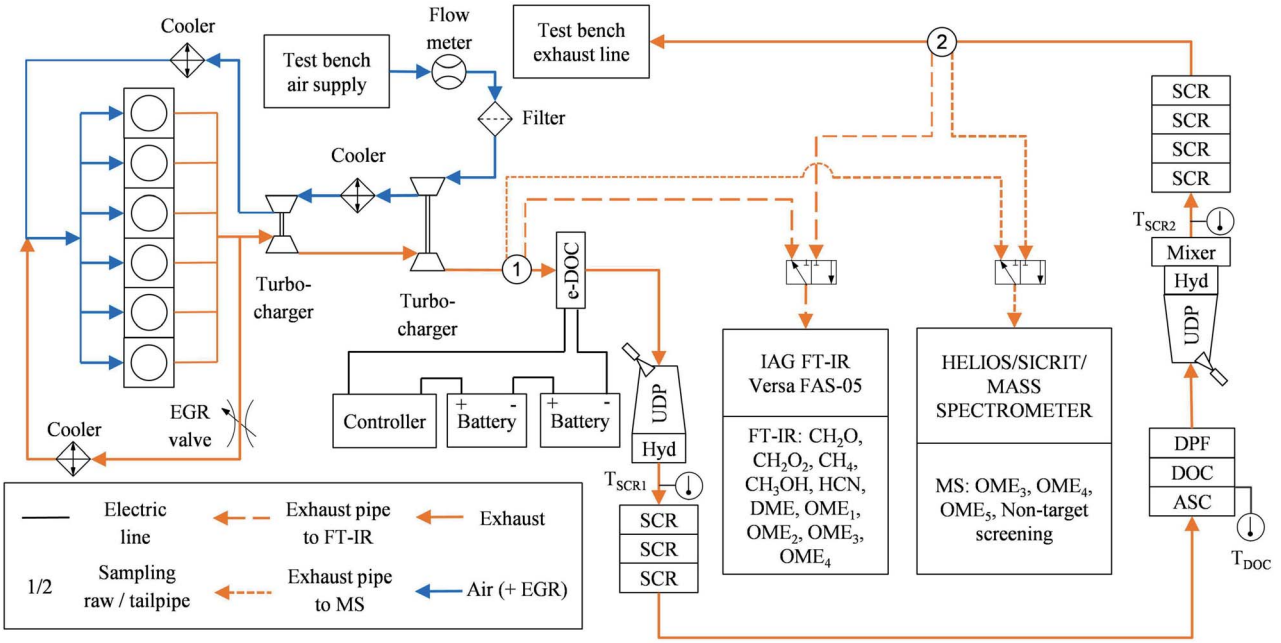

Fig. 1 Test bench setup.

2–4 (OME_2, OME_3, OME_4). Different OME in the exhaust indicate an incomplete combustion, as well as CH_3OH and CH_2O, since they are reactants in OME synthesis.[39] The FT-IR has a standard calibration. Therefore, the detection limits of the chemical species of interest are limited to the general specifications of the manufacturer. Table 2 in the ESI† lists the detection limits of interest. Two sampling points located downstream of the second turbocharger (raw exhaust) and downstream of the second SCR stage (tailpipe exhaust) were utilized for the exhaust samples analyzed using the FT-IR. A 3/2-way solenoid valve enabled switching between the two sampling points.

HELIOS/SICRIT/mass spectrometer

In addition to the FT-IR, the exhaust from the two sampling points was analyzed using the custom-built Mass spectrometer (MS) system described by Thaler *et al.*[46] In short, the MS was composed of a Thermo Fin Finnigan LTQ ion trap mass spectrometer by Thermo Fisher Scientific Inc. (Germany) with a commercially available highly efficient atmospheric ionization source named "soft-ionization by chemical reaction in transfer (SICRIT)" by Plasmion GmbH (Germany).[47] Directly upstream of the SICRIT ion source, a custom-built "high efficient light source for optical surface desorption (HELIOS)" infrared oven was used for evaporation of volatile particle components, thus enabling online detection of both gaseous exhaust species and volatile and semi-volatile aerosols or species absorbed on solid particles. The exhaust samples entered the HELIOS oven through stainless steel tubing heated to 191 °C and diluted by 20% with humidified nitrogen.

Fig. 2a shows a typical mass spectrum of the ambient temperature head space of the OME fuel mixture measured using the MS system. Major mass peaks were at m/z 154, 184, and 214, which correspond to OME_3, OME_4, and OME_5, respectively. These peaks were at [M + 18], where M is the molecular mass of the respective OME_n. The elemental composition of the [M + 18] signal was determined as [M + NH_4^+] with mass deviations below 2 ppm. NH_4^+-adducts were further confirmed by the [M + 22] signal corresponding to [M + ND_4^+] when measured with nitrogen humidified with deuterium oxide (D_2O). Fig. 1 in the ESI† contains this measurement by means of a different high-resolution mass spectrometer (Thermo LTQ Orbitrap XL) coupled with the SICRIT ion source.

Calibration of the HELIOS/SICRIT/MS system for OME was performed in the laboratory using samples of OME_3, OME_4, and OME_5 each, all supplied by ASG Analytik-Service AG. Two different methods were used to introduce known concentrations of each OME into the MS system. The first method utilized a syringe pump (Pico Plus Elite, Harvard Apparatus) for injecting each OME in liquid form into a vaporizer, which was built in-house and was similar to the one described by Herrmann *et al.*[48] The vaporized OME was diluted with humidified nitrogen obtained by bubbling nitrogen (purity 5.0) through a flask filled with distilled water. The nitrogen flow rate was controlled with mass flow controller (Vögtlin red-y smart controller GSC). The second method for introducing known concentrations of OME into the MS system involved the same syringe pump, but, instead of liquid OME the headspace of each OME from a headspace vial was injected into a stream of humidified nitrogen. The concentration of OME in the headspace was determined based on the vapor pressure of each OME as given by Boyd.[49] Both methods yielded consistent signals as measured by the MS system. The measured intensity at the respective mass peak for OME_3, OME_4 and OME_5 are shown in Fig. 2b, which shows the calibration coefficients along with the

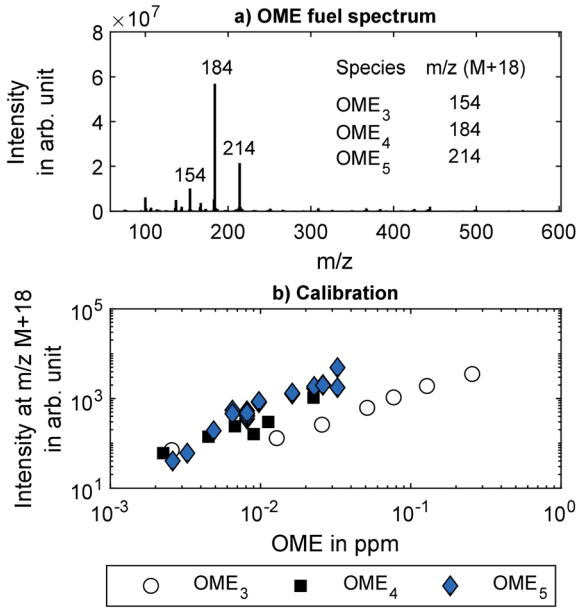

Species	ppm/intensity	σ
OME_3	$7.5471 \cdot 10^{-5}$	$2.1261 \cdot 10^{-5}$
OME_4	$3.5483 \cdot 10^{-5}$	$1.1881 \cdot 10^{-5}$
OME_5	$1.9514 \cdot 10^{-5}$	$1.4150 \cdot 10^{-5}$

Fig. 2 (a) Mass spectrum of OME fuel mixture. (b) Calibration results of the MS used for several polyoxymethylene dimethyl ethers. The calibration factor for each OME is also given, where σ describes the standard deviation of the calibration factor over the multiple measurements. The intensity is given in arbitrary units.

estimated uncertainty. These calibration coefficients were used to quantify the OME concentration in the engine experiments. No calibration was performed for OME_6 because its solid form at room temperature could not be introduced into the syringe pump, and its vapor pressure was too low to recover a sufficiently high concentration from a headspace vial. However, based on the high-resolution mass spectrometer measurements, the mass peak from OME_6 can be expected at m/z 244.

In the engine experiments, the HELIOS/SICRIT/MS system enabled non-target screening for unknown components in the exhaust samples that were not configured in the FT-IR. The MS system can detect only species with a mass-to-charge ratio over m/z 50, meaning that lighter chemical species such as CH_4 and CH_2O cannot be detected. The detection limit of the MS system for heavier species, such as OME, is lower than that of the FT-IR employed in this study. The detection limits of the MS system were found to be 20 ppb, 9 ppb, and 2 ppb for OME_3, OME_4 and OME_5, respectively, which are orders of magnitude lower than the detection limits of the OME concentrations using the FT-IR, as listed in Table 2 in the ESI†.

Test procedure

The test cycle used to investigate the cold-start emissions in OME engine operation was the WHTC, in accordance with UN/ECE Regulation No. 49.[50] The cycle starts at ambient conditions. Since the procedure stipulates that there must be no preconditioning, the various test runs were carried out over the course of several days. The ambient temperatures at all times were approximately 29 °C, with daily deviations of less than 1 °C. After the initial test run, the engine was shut off for a waiting period of ten minutes before starting the next run. In this study, the first and the second run are referred to as "cold" and "hot" runs, respectively. After each hot cycle, the engine performed a clearing out of the SCR system without urea dosage, so every cold run, including the initial one, started with empty ammonia storage of the catalysts. Test runs using the e-DOC start with immediate power supply of the heating disc after start of engine operation. After 20 minutes, the power supply was switched off.

For the application of fuel dosing, the engine used the engine control unit's DPF regeneration mode. In this case, a late post injection (PoI) at 120° crank angle provided fuel for the exothermic reaction at the DOC in a manner similar to the experiments in the previous study.[31] The quantity of PoI (qPoI) in gravimetric diesel equivalent was set to 15 mg/str, which corresponds to about 33.75 mg/str of OME.

During the hot run of the WHTC, both fuel dosing and the e-DOC power supply were switched off.

Since the modular ATS consists of monolithic discs connected *via* flanges and pipes, the heat losses were particularly higher than in a configuration with standard integration in a thermally insulated silencer. Therefore, the evaluation of the effectiveness in heating behavior is limited to qualitative statements in this study.

Results and discussion

OME concentration in engine exhaust determined *via* mass spectrometry

An initial investigation of the engine emissions during the WHTC was performed without applying any methods of ATS heating. In this context, Fig. 3 compares the concentration of OME_3, OME_4, and OME_5 in the engine exhaust during the cold and hot WHTC runs at the raw exhaust and tailpipe exhaust sampling positions, as determined by the MS system. The concentration of OME_3 was the lowest, with a maximum value of 5 ppm overall. OME_3 has the lowest boiling point of the monitored OME_n. For this reason, the evaporation tendency of OME_3 is expected to be higher, especially towards the end of the combustion. According to the property values determined by Lautenschütz *et al.*,[36] the Weber number decreases with increasing OME_n chain length. This dimensionless number describes the fuel droplet decomposition during the injection by putting the drag force and cohesion force on the interface of two different fluids in proportion. The decreasing Weber number indicates a reduced droplet decay with increasing OME_n chain length. The ignitibility is to be excluded as a causal factor because it increases with the chain length of OME_n.[36,51] The maximum values of the OME_4 and OME_5 concentrations were 36 ppm and 35 ppm, respectively. The difference between the cold and hot runs was marginal for all three species,

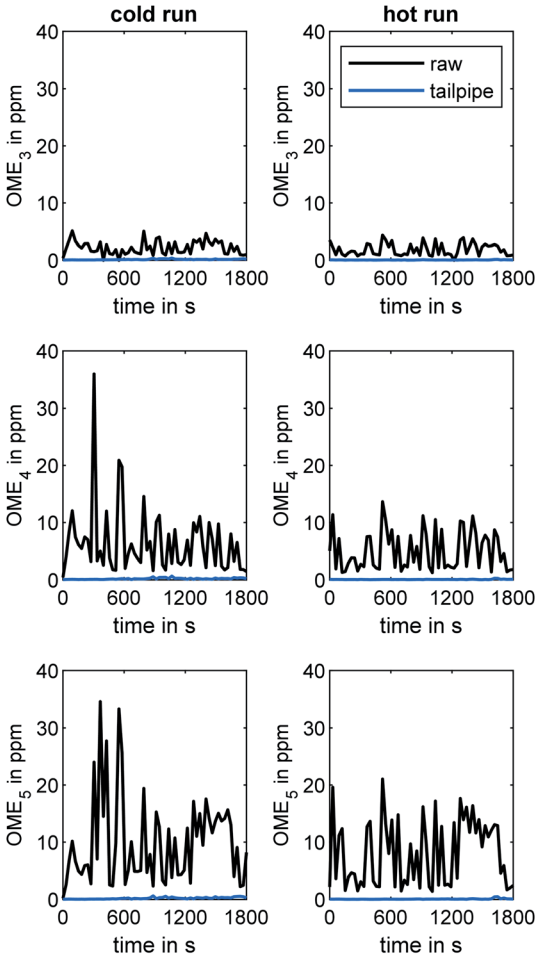

Fig. 3 Concentrations of OME_3, OME_4, and OME_5 in the engine exhaust during the WHTC cold and hot runs at the two sampling positions (raw and tailpipe sampling).

although the peak concentration of OME_4 and OME_5 in the raw exhaust was higher during the cold run. However, the difference between raw and tailpipe sampling is clearer than the difference between the cold and hot runs. Whereas the concentrations of all three OME species were in the range of several ppm in the raw exhaust, the concentrations did not exceed 1 ppm for any of the species when analyzed at the tailpipe position. Elsener *et al.* demonstrated the high hydrolysis activity of OME_3 on several catalytic surfaces.[52] Therefore, adsorption and reaction *via* hydrolysis or oxidation during the flow through the ATS was likely, since the ATS contained two TiO_2 catalysts and three Pt(-Pd)-coated catalysts.

Non-target screening

Fig. 4 shows the mass spectra at all times during the WHTC cold and hot test runs, presenting the results of the non-target screening analysis.

Like in Fig. 3, clear differences between raw and tailpipe emissions appear, whereas the differences between the cold and hot runs at both sampling positions were not clearly differentiable. At the raw exhaust position, intensity maxima are seen at

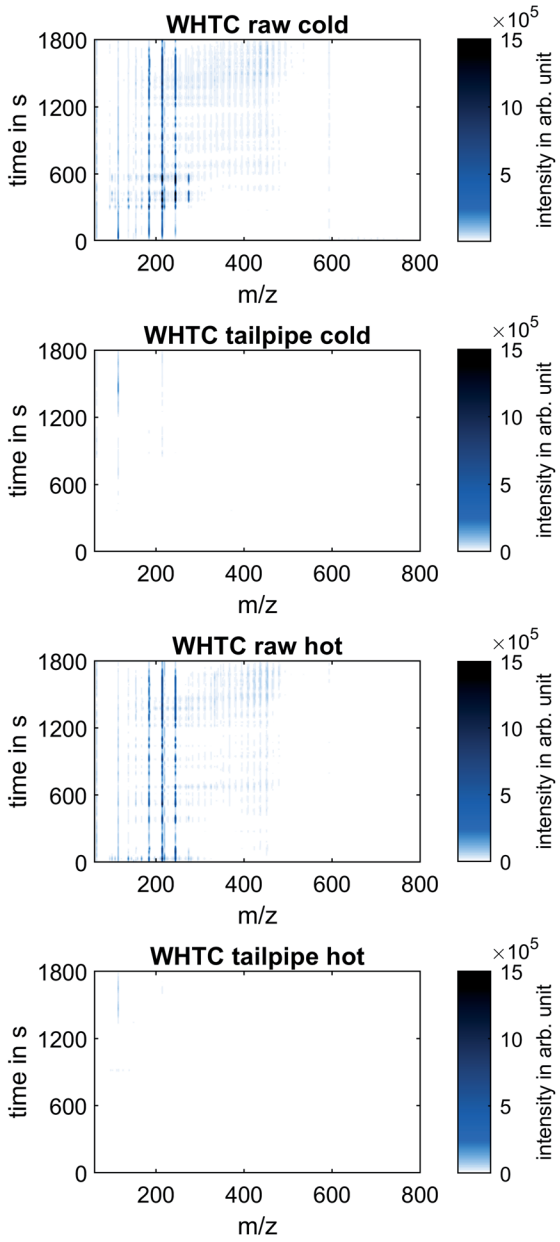

Fig. 4 Mass spectra of the non-target screening analysis with the maximum peaks of the sample from the raw exhaust shown at the *m*/*z* values corresponding to OME_4, OME_5, and OME_6. The intensity is given in arbitrary unit.

m/*z* 184, 214, and 244, suggesting that of OME_4, OME_5, and OME_6 formed the majority of the high-mass species in the exhaust gas. During the cold run, mass peaks also appeared at *m*/*z* 124 and *m*/*z* 274 in the raw exhaust, indicating the presence of OME_2 and OME_7 as well. In both the cold and the hot run, intensity peaks at *m*/*z* 114 stood out from the rest of the spectra at the tailpipe position towards the end of the WHTC, after approximately 1200 seconds. The high signal at *m*/*z* 114 was more pronounced in cold operation than in hot operation. In both cases, however, the maximum intensity of the *m*/*z* 114 trace was an order of magnitude lower than the signal intensity

of the mass peaks corresponding to unburned OME. Although the identity of the species generating the mass peak at m/z 114 was not able to be determined with the current MS system (a higher resolution mass spectrometer would be needed), the mass peak at m/z 114 has appeared in measurements in the same engine operated using fossil diesel fuel. Therefore, this substance is unlikely to be an unknown product of OME combustion, but further identification of this peak remains necessary. In summary, the mass spectra from both the cold and the hot runs, as well as both the raw exhaust and tailpipe exhaust sampling positions over the entire range of measured mass-to-charge ratios and measurement time, showed no signal intensities on a similar order of magnitude as the detected unburned OME in the raw exhaust. This result justifies the following focus on lightweight species known to occur in OME combustion, which include CH_2O, CH_4 and HCN as byproducts in exhaust after-treatment. The concentration of these species can be determined by means of the FT-IR.

Gaseous emissions determined *via* FT-IR

Fig. 5 presents the concentration of key species in the tailpipe exhaust measured with FT-IR during both WHTC runs. As already revealed by Gelner *et al.*, a higher EGR valve dynamic leads to CH_4 concentration peaks in the exhaust, due to the CH_4-NO_x-trade-off in an OME engine.[19] The CH_4 concentration peaks are more frequent during hot operation because the EGR valve remains closed during the cold-start operation. However, the integrated cycle result of the hot run regarding CH_4 concentration in the tailpipe exhaust is 7 ppm. Reduction of the concentration of CH_4 in future OME engine application would be desirable since CH_4 is a greenhouse gas.[1,53] CH_2O emission was also of interest in this study given its toxic effect on human health.[54] The effect of a hot ATS is clear from the results in Fig. 5. Whereas CH_2O appeared at concentrations of up to 41 ppm after a cold ATS during the cold run, the maximum value of the peak CH_2O concentration during hot operation was only 17 ppm. The WHTC cycle evaluation results were 9 ppm in cold operation and 1 ppm in hot operation. The exhaust concentration of CH_2O_2 – the first oxidation stage of CH_2O – exhibited the same behavior as seen with CH_2O, but at lower concentrations. The measured HCN concentration remained under 1.2 ppm in cold-start operation and was slightly lower in hot operation. The higher signal in the first part of the cold run may have been caused by the formation of small amounts of HCN due to residues of NH_3 on the SCR catalyst,[29] remaining after the clearing process prior to the test run. The effect of HCN formation might be more pronounced in repeated runs with cold-start operation occurring in road operation without clearing procedures. Furthermore, an investigation of intermediate products, as observed by Nuguid *et al.*,[55] would be necessary in order to generate a full assessment of the processes in the SCR system. However, since the HCN concentration signal was below the general FT-IR detection limit of 1.5 ppm provided by the manufacturer in Table 2 in the ESI†, the strategy of combining oxidative catalysts upstream and downstream of the SCR stage proved to be effective.

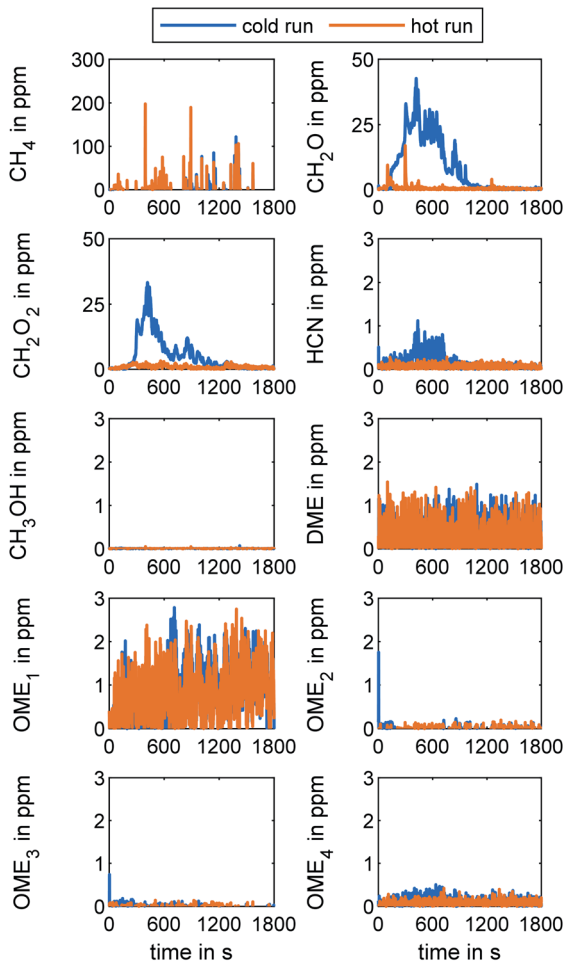

Fig. 5 Gaseous tailpipe emissions during WHTC cycle determined *via* FT-IR.

Regarding CH_3OH, DME, and OME_{1-4} as precursors of incomplete OME combustion, the tailpipe concentration was below 3 ppm regardless of cold or hot operation. This result agreed with the measurements using the MS system shown in Fig. 3. Gaiser *et al.* observed high concentrations of ethanol during OME combustion, as well as acetaldehyde and methyl formate.[56] The FT-IR used in this work did not include this species in the specific method, so further investigations regarding the products of incomplete OME combustion in addition to CH_4, CH_3OH, CH_2O, CH_2O_2, and OME_{0-6} will be necessary.

Since the concentration of CH_2O, CH_2O_2, and HCN in the exhaust were all higher in cold-start operation than in the hot run, methods for reducing the duration of the ATS heating period when the catalysts are below their light-off temperature are essential to reducing the overall concentration of these species during typical on-road engine operation. Furthermore, NO_x reduction *via* SCR also requires an operational hot system for urea dosing.

After-treatment system heating

Four cold runs of the WHTC comprised the current study on ATS heating methods. A run without an e-DOC served as

a baseline and enabled qualitative evaluation of the effectiveness of three different ATS heating methods. For the baseline run, the e-DOC was removed completely. The three runs using the electrical heating function of the e-DOC differed in PoI strategy: one run was without PoI, one run was with a PoI start at a temperature downstream of the first Hyd of $T_{SCR1} = 230$ °C, and one run had a later PoI start at a temperature of $T_{SCR1} = 280$ °C. The PoI ended at a temperature of the second SCR stage of $T_{SCR2} = 230$ °C. Fig. 6 depicts the results for the four runs using different ATS heating methods. The different path lengths to the respective catalysts delayed the heating effects of the various ATS heating methods. Whereas the energization of the e-DOC was noticeable by a temperature difference of 20 °C at the point of T_{SCR1} after 129 s, T_{SCR2} reached this value after 1146 s. After 635 s, the PoI with the threshold from $T_{SCR1} = 230$ °C started and the PoI with the threshold from $T_{SCR1} = 280$ °C started after 837 s. The run with the earlier PoI reached the termination criterion for the PoI ($T_{SCR2} = 230$ °C) after 1012 s, and the run with a later PoI did so after 1095 s. The run having only the e-DOC energized reached this temperature level after 1587 s. The run with lower temperature threshold for start of PoI generated a higher CH_2O slip through the ATS than the other runs. The CH_2O concentration of the run with a higher temperature threshold was at the level of the runs without PoI. In this run, at the beginning of fuel dosing, the temperature level upstream of the two DOCs was higher, so the catalytic conversion of CH_2O formed by PoI was higher.[31] A later start of fuel dosing thus reduced the length of the cold-start phase without additional CH_2O slip, albeit with a higher heating time than in a run with earlier start of PoI.

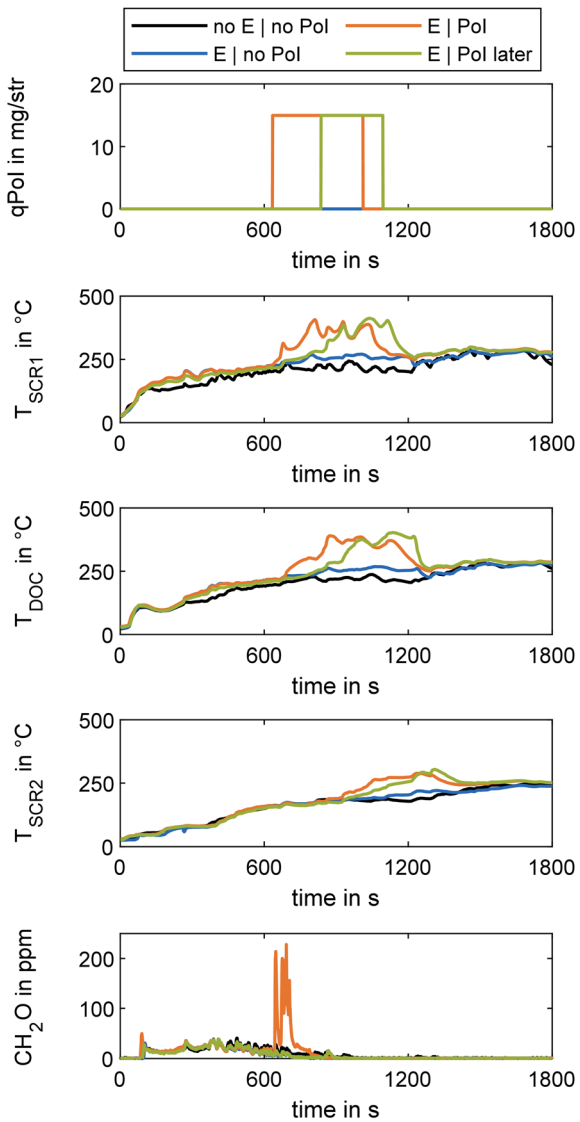

Fig. 6 Comparison of different ATS temperatures using different measures of ATS heating. qPoI is given in gravimetric diesel equivalent; temperatures of the catalysts determined *via* thermocouples; CH_2O determined *via* FT-IR at tailpipe position. e-DOC electrification starts with engine start and ends after 20 minutes. PoI starts at $T_{SCR1} = 230$ °C and 280 °C respectively. PoI ends at $T_{SCR2} = 230$ °C.

Table 4 Reduction of NO_x exhaust concentration during WHTC procedure due to the respective ATS heating method, as compared to the baseline measurement. The overall evaluation includes weighting of cold and hot run in accordance to UN/ECE R49[50]

NO_x emissions reduction in WHTC	Cold run	Overall evaluation
Without e-DOC	Baseline	Baseline
With e-DOC | No PoI	22.7%	47.7%
With e-DOC | PoI 230 °C	41.3%	64.9%
With e-DOC | PoI 280 °C	36.0%	61.8%

Table 4 shows the respective reduction of NO_x emission concentration levels for three different ATS heating methods. The reduction is provided in comparison to the baseline cold run and the overall evaluation of the WHTC for both baseline cold run and baseline hot run without ATS heating, respectively. The result of the WHTC evaluation, in mg kW^{-1} h^{-1}, was in accordance with UN/ECE R49.[50] This data enables evaluation of the effect of the ATS heating methods regarding NO_x reduction of the SCR system, due to higher efficiency and an earlier start of urea dosing.

Using e-DOC energizing and fuel dosing with a start of PoI at $T_{SCR1} = 230$ °C reduced the NO_x emissions by 41.3% as compared to the baseline cold run. Due to the higher temperature of the ATS at the start of the hot run, this reduced the overall NO_x concentration in the exhaust during the overall WHTC procedure by 64.9%. This reduction comes at a cost of a higher CH_2O concentration of 90.5% in the cold run and 58.3% overall, as compared to the baseline. A later start of fuel dosing enables a 36.0% reduction of NO_x as compared to the baseline cold run and a 61.8% reduction overall; the rise in CH_2O concentration is below 4.8% in comparison to the baseline cold run and below 0.1% in comparison to the overall evaluation and, therefore negligible. Single use of the e-DOC reduces NO_x emissions by 22.7% and 47.7% as compared to the baseline cold run and overall, respectively. Since the heat losses of the ATS in the modular configuration used in this work were higher than with a thermally insulated silencer, the advantages in a system ready for series production are assumed to be higher.

Conclusions and outlook

The present work contains experimental studies on the gaseous emissions and effectiveness of ATS heating measures during cold-start operation of a heavy-duty engine fueled with OME.

Measurements from the MS system of the concentration of different OME chain lengths in the raw and tailpipe exhaust enable evaluation of the effectiveness of the ATS in cold-start and hot-start operation. A non-target screening analysis performed using the same MS system suggests that no unknown heavy species derived from the combustion of OME were present in the exhaust gas at similar levels to the unburned OME. Concentration measurements of key species using the FT-IR reveal the differences between cold-start and hot-start transient operation. The comparison of the use of an electrical heatable DOC and fuel dosing clarifies the potential of methods to reduce the length of the cold-start phase. The results are summed up in the following conclusions:

In both the cold and hot operation during the WHTC, the concentration of OME_3, OME_4, and OME_5 measured with the calibrated MS system in the tailpipe exhaust do not exceed 1 ppm. The authors assume that adsorption, hydrolysis, and oxidation processes in the ATS are responsible for this result.

The non-target screening analysis *via* the MS system confirmed that the most dominant species in the exhaust are OME_n. No partially oxidized products were present in the exhaust at levels on the same order of magnitude. This result justifies a focus on the known pollutant emissions formed in OME exhaust such as CH_4 or CH_2O.

In both cold and hot operation, the tailpipe concentration of HCN remains below the given detection limit of the FT-IR used. Further experiments will be necessary in order to evaluate the processes during on-road operation, as well as using different SCR configurations. Differences in the performance of the CuZe catalysts used and SCR catalysts based on vanadium may occur in addition to differences due to different ammonia storage levels of the catalyst.

During cold-start operation, an engine fueled with OME primarily emits, besides NO_x, CH_2O and CH_2O_2 as long as the oxidation activity of the catalysts is inhibited. Further research on the formation processes of these species and in-engine methods for reducing the concentration of these species is necessary.

Fuel dosing in combination with an electrically heatable DOC is an effective method of shortening the cold-start phase in OME operation and enables earlier start of urea dosing and therefore NO_x reduction. An early start of fuel dosing with inhibited oxidation activity of the catalysts due to lower temperature leads to a CH_2O slip. Avoidance of the slip is possible by a later fuel dosing start but at the cost of a later NO_x reduction start.

By means of the configuration in this study, the NO_x emissions during a WHTC procedure are reduced by 64.9% using an e-DOC and fuel dosing, but with a CH_2O increase of 58.3%. With an increase in CH_2O emission of less than 0.1%, the NO_x reduction is 61.8%. Operation with the e-DOC without PoI enables a reduction in NO_x emission by 47.7%.

These conclusions are based on the experimental results of this work. Further studies will be necessary in order to validate the observed behavior and reduction potential with a thermally insulated ATS in a silencer. Furthermore, the potential of OME regarding NO_x reduction by way of an applied EGR strategy[19] and the increase in SCR performance by fuel dosing and electrical heating demonstrated in this work enable simplification of the ATS back to a one-stage SCR system, thus improving economic efficiency. Additionally, omission of the DPF by virtue of the low particle emission of an OME engine[57] reduces complexity and offers advantages in the cold-start phase with respect to ATS heating. Since the experiments in this study took place during summer at moderate ambient temperatures, further experiments with lower starting temperatures – *e.g.* temperatures below 0 °C – will be necessary for a holistic approach. Furthermore, the interactions of OME with components in contact with fuel should be investigated with regard to corrosion in long-term studies. Jin *et al.* observed increasing corrosion with increasing amounts of OME in a blend with methanol, palm oil and palm kernel oil.[58]

Author contributions

Alexander D. Gelner: conceptualization, data curation, formal analysis, investigation, methodology, project administration, validation, visualization, writing – original draft, writing – review & editing. Genny A. Pang: conceptualization, data curation, formal analysis, investigation, methodology, validation, writing – original draft, writing – review & editing. Christoph Haisch: conceptualization, funding acquisition, project administration, supervision, writing – review & editing. Harald A. Beck: validation, formal analysis, data curation, writing – review & editing. Christian Pastoetter: conceptualization, funding acquisition, project administration, supervision, writing – review & editing. Martin Härtl: funding acquisition, project administration, supervision, writing – review & editing. Malte Jaensch: writing – review & editing. Georg Wachtmeister: funding acquisition, project administration, supervision, writing – review & editing.

Conflicts of interest

The authors declare that they have no known competing financial interests or personal relationship that could have appeared to influence the work reports in this paper.

Definitions and abbreviations

ASC	ammonia slip catalyst
ATS	after-treatment system
BHT	butylated hydroxytoluene
CuZe	copper zeolite
DME	dimethyl ether (OME_0)
DOC	diesel oxidation catalyst

DPF	diesel particulate filter
e-DOC	electrically heatable diesel oxidation catalyst
FAME	fatty acid methyl esters
FT-IR	Fourier-transform infrared spectrometer
HELIOS	high efficient light source for optical surface desorption
Hyd	hydrolysis catalyst
LHV	lower heating value
MS	mass spectrometer
OFA	open frontal area
OME	polyoxymethylene dimethyl ethers
OME_1	methylal (dimethoxymethane)
OMEn	polyoxymethylene dimethyl ether of the chain length n
PGM	platinum group metals
PoI	post injection
ppm	parts per million
qPoI	quantity of post injection
SCR	selective catalytic reduction
SICRIT	soft-ionization by chemical reaction in transfer
UDP	Universal Decomposition Pipe
WHTC	World Harmonized Transient Cycle
σ	standard deviation

Acknowledgements

The research was part of the project "Sub-Zero-Emissions Dieselmotor", funded by the Bavarian Research Foundation (grant number AZ-1266-17). The project was carried out in collaboration with MAN Truck & Bus SE, VT Vitesco Technologies Emitec GmbH, Chair of Analytical Chemistry of TUM and ASG Analytik-Service AG. Their support is gratefully acknowledged. The authors also want to thank Dr Dieter Rothe, Dipl.-Ing. Florian Lindner (both MAN Truck & Bus SE) and Martin Elsener (Paul Scherrer Institute) for their support and consultation in this study.

References

1 *Climate change 2014: Synthesis report*, ed. Pachauri RK and Meyer L, Intergovernmental Panel on Climate Change, Geneva, Switzerland, 2015.
2 *Renewable Energy Sources and Climate Change Mitigation: Special Report of the Intergovernmental Panel on Climate Change*, ed. Edenhofer O, Pichs-Madruga R and Sokona Y, Intergovernmental Panel on Climate Change, 2012.
3 S. Schemme, J. L. Breuer, M. Köller, S. Meschede, F. Walman, R. C. Samsun, *et al.* H2-based synthetic fuels: A techno-economic comparison of alcohol, ether and hydrocarbon production, *Int. J. Hydrogen Energy*, 2020, **45**(8), 5395–5414.
4 M. Härtl, P. Seidenspinner, E. Jacob and G. Wachtmeister, Oxygenate screening on a heavy-duty diesel engine and emission characteristics of highly oxygenated oxymethylene ether fuel OME1, *Fuel*, 2015, **153**, 328–335.
5 S. Schemme, R. C. Samsun, R. Peters and D. Stolten, Power-to-fuel as a key to sustainable transport systems – An analysis of diesel fuels produced from CO 2 and renewable electricity, *Fuel*, 2017, **205**, 198–221.
6 M. Held, Y. Tönges, D. Pélerin, M. Härtl, G. Wachtmeister and J. Burger, On the energetic efficiency of producing polyoxymethylene dimethyl ethers from CO 2 using electrical energy, *Energy Environ. Sci.*, 2019, **12**(3), 1019–1034.
7 L. Pellegrini, M. Marchionna, R. Patrini, C. Beatrice, N. Del Giacomo, and C. Guido. Combustion Behaviour and Emission Performance of Neat and Blended Polyoxymethylene Dimethyl Ethers in a Light-Duty Diesel Engine, in, *SAE Technical Paper Series. SAE International400 Commonwealth Drive*, Warrendale, PA, United States, 2012, SAE Technical Paper Series.
8 L. Pellegrini, M. Marchionna, R. Patrini and S. Florio. Emission Performance of Neat and Blended Polyoxymethylene Dimethyl Ethers in an Old Light-Duty Diesel Car, in, *SAE Technical Paper Series. SAE International400 Commonwealth Drive*, Warrendale, PA, United States, 2013, SAE Technical Paper Series.
9 S. E. Iannuzzi, C. Barro, K. Boulouchos and J. Burger, Combustion behavior and soot formation/oxidation of oxygenated fuels in a cylindrical constant volume chamber, *Fuel*, 2016, **167**, 49–59.
10 A. Damyanov, P. Hofmann, B. Geringer, N. Schwaiger, T. Pichler and M. Siebenhofer, Biogenous ethers: production and operation in a diesel engine, *Automot. Engine Technol.*, 2018, **3**(1–2), 69–82.
11 H. Ogawa, N. Miyamoto, M. Yagi. Chemical-Kinetic Analysis on PAH Formation Mechanisms of Oxygenated Fuels. in: *SAE Technical Paper Series. SAE International400 Commonwealth Drive*, Warrendale, PA, United States, 2003, SAE Technical Paper Series.
12 C. J. L. Murray, A. Y. Aravkin, P. Zheng, C. Abbafati, K. M. Abbas, M. Abbasi-Kangevari, *et al.* Global burden of 87 risk factors in 204 countries and territories, 1990–2019: a systematic analysis for the Global Burden of Disease Study 2019, *Lancet*, 2020, **396**(10258), 1223–1249.
13 T. C. Bond, S. J. Doherty, D. W. Fahey, P. M. Forster, T. Berntsen, B. J. DeAngelo, *et al.* Bounding the role of black carbon in the climate system: A scientific assessment, *J. Geophys. Res.: Atmos.*, 2013, **118**(11), 5380–5552.
14 D. Pélerin, K. Gaukel, M. Härtl, E. Jacob and G. Wachtmeister, Potentials to simplify the engine system using the alternative diesel fuels oxymethylene ether OME1 and OME3−6 on a heavy-duty engine, *Fuel*, 2020, **259**, 116231.
15 D. Pélerin, K. Gaukel, M. Härtl, G. Wachtmeister. Nitrogen Oxide Reduction Potentials Using Dimethyl Ether and Oxymethylene Ether in a Heavy-Duty Diesel Engine, in, *SAE Technical Paper Series. SAE International400 Commonwealth Drive*, Warrendale, PA, United States; 2020, SAE Technical Paper Series.
16 S. Pöllmann, M. Härtl and G. Wachtmeister, Potential of miller timing with synthetic diesel fuels on a single cylinder heavy-duty engine, *Int. J. Engine Res.*, 2021, 146808742110436.

17 B. Gaston, J. M. Drazen, J. Loscalzo and J. S. Stamler, The biology of nitrogen oxides in the airways, *Am. J. Respir. Crit. Care Med.*, 1994, **149**(2 Pt 1), 538–551.
18 K. Li, L. Chen, S. J. White, K. Han, B. Lv, K. Bao, *et al.* Effect of nitrogen oxides (NO and NO 2) and toluene on SO 2 photooxidation, nucleation and growth: A smog chamber study, *Atmos. Res.*, 2017, **192**, 38–47.
19 A. D. Gelner, H. A. Beck, C. Pastoetter, M. Härtl and G. Wachtmeister, Ultra-low emissions of a heavy-duty engine powered with oxymethylene ethers (OME) under stationary and transient driving conditions, *Int. J. Engine Res.*, 2021, 146808742110479.
20 L. Yang, V. Franco, P. Mock, R. Kolke, S. Zhang, Y. Wu, *et al.* Experimental Assessment of NOx Emissions from 73 Euro 6 Diesel Passenger Cars, *Environ. Sci. Technol.*, 2015, **49**(24), 14409–14415.
21 R. Williams, J. Andersson, H. Hamje, P. Ziman, K. Kar and C. Fittavolini *et al.* Impact of Demanding Low Temperature Urban Operation on the Real Driving Emissions Performance of Three European Diesel Passenger Cars, in, *SAE Technical Paper Series. SAE International400 Commonwealth Drive*, Warrendale, PA, United States, 2018, SAE Technical Paper Series.
22 C. Dardiotis, G. Martini, A. Marotta and U. Manfredi, Low-temperature cold-start gaseous emissions of late technology passenger cars, *Atmos. Res.*, 2013, **111**, 468–478.
23 A. Broatch, B. Tormos, P. Olmeda and R. Novella, Impact of biodiesel fuel on cold starting of automotive direct injection diesel engines, *Energy*, 2014, **73**, 653–660.
24 M. Weilenmann, P. Soltic, C. Saxer, A.-M. Forss and N. Heeb, Regulated and nonregulated diesel and gasoline cold start emissions at different temperatures, *Atmos. Environ.*, 2005, **39**(13), 2433–2441.
25 A. S. Ramadhas and H. Xu, Cold start particle number, size and mass emissions from a CRDI diesel engine running on biodiesel blends in a cold environment, *Biofuels*, 2016, **7**(4), 353–363.
26 R. Suarez-Bertoa and C. Astorga, Impact of cold temperature on Euro 6 passenger car emissions, *Environ. Pollut.*, 2018, **234**, 318–329.
27 C. Barro, M. Parravicini, K. Boulouchos and A. Liati, Neat polyoxymethylene dimethyl ether in a diesel engine; part 2: Exhaust emission analysis, *Fuel*, 2018, **234**, 1414–1421.
28 D. Zengel, P. Koch, B. Torkashvand, J.-D. Grunwaldt, M. Casapu and O. Deutschmann, Emission of Toxic HCN During NOx Removal by Ammonia SCR in the Exhaust of Lean-Burn Natural Gas Engines, *Angew. Chem., Int. Ed. Engl.*, 2020, **59**(34), 14423–14428.
29 M. Elsener, R. J. G. Nuguid, O. Kröcher and D. Ferri, HCN production from formaldehyde during the selective catalytic reduction of NOx with NH3 over V2O5/WO3-TiO2, *Appl. Catal., B*, 2021, **281**, 119462.
30 J. Gao, G. Tian, A. Sorniotti, A. E. Karci and R. Di Palo, Review of thermal management of catalytic converters to decrease engine emissions during cold start and warm up, *Appl. Therm. Eng.*, 2019, **147**, 177–187.
31 A. D. Gelner, C. Pastoetter, H. A. Beck, M. Härtl, G. Wachtmeister Fuel Dosing on a Diesel Oxidation Catalyst for After-Treatment System Heating on a Heavy-Duty Engine Powered by Polyoxymethylene Dimethyl Ethers, in, *SAE Technical Paper Series. SAE International400 Commonwealth Drive*, Warrendale, PA, United States, 2020, SAE Technical Paper Series.
32 K. Nakano, H. Okano, K. Inoue, A. Obuchi Study on the Prevention of Face-Plugging of Diesel Oxidation Catalyst (DOC), in, *SAE Technical Paper Series. SAE International400 Commonwealth Drive*, Warrendale, PA, United States, 2018, SAE Technical Paper Series.
33 W. Maus, R. Brück, R. Konieczny and A. Scheeder, Electrically heated catalyst for thermal management in modern vehicle applications, *MTZ Worldw*, 2010, **71**(5), 34–39.
34 DIN/TS 51699 – Fuels – Polyoxymethylene dimethyl ether (OME): Draft German Standard.
35 *DIN EN 590:2017-10, Kraftstoffe_- Dieselkraftstoff_- Anforderungen und Prüfverfahren; Deutsche Fassung EN_590:2013+A1:2017*. Berlin: Beuth Verlag GmbH.
36 L. Lautenschütz, D. Oestreich, P. Seidenspinner, U. Arnold, E. Dinjus and J. Sauer, Physico-chemical properties and fuel characteristics of oxymethylene dialkyl ethers, *Fuel*, 2016, **173**, 129–137.
37 S. K. Hoekman, A. Broch, C. Robbins, E. Ceniceros and M. Natarajan, Review of biodiesel composition, properties, and specifications, *Renewable Sustainable Energy Rev.*, 2012, **16**(1), 143–169.
38 A. D. Gelner, R. Höß, A. Zepf, M. Härtl, G. Wachtmeister. Engine Operation Strategies for the Alternative Diesel Fuel Oxymethylene Ether (OME): Evaluation Based on Injection Rate Analyzer and 0D-/1D-Simulation, in, *SAE Technical Paper Series. SAE International400 Commonwealth Drive*, Warrendale, PA, United States, 2021, SAE Technical Paper Series.
39 J. Burger, M. Siegert, E. Ströfer and H. Hasse, Poly(oxymethylene) dimethyl ethers as components of tailored diesel fuel: Properties, synthesis and purification concepts, *Fuel*, 2010, **89**(11), 3315–3319.
40 I. Bogatykh, T. Osterland, H. Stein and T. Wilharm, Investigation of the Oxidative Degradation of the Synthetic Fuel Oxymethylene Dimethyl Ether, *Energy Fuels*, 2020, **34**(3), 3357–3366.
41 C. Barro, M. Parravicini and K. Boulouchos, Neat polyoxymethylene dimethyl ether in a diesel engine; part 1: Detailed combustion analysis, *Fuel*, 2019, **256**, 115892.
42 S. D. Yim, S. J. Kim, J. H. Baik, I. Nam, Y. S. Mok, J.-H. Lee, *et al.* Decomposition of Urea into NH 3 for the SCR Process, *Ind. Eng. Chem. Res.*, 2004, **43**(16), 4856–4863.
43 M. Koebel, M. Elsener and T. Marti, NO x -Reduction in Diesel Exhaust Gas with Urea and Selective Catalytic Reduction, *Combust. Sci. Technol.*, 1996, **121**(1–6), 85–102.
44 K. Kamasamudram, C. Henry, N. Currier and A. Yezerets, N 2 O Formation and Mitigation in Diesel Aftertreatment Systems, *SAE Int. J. Engines*, 2012, **5**(2), 688–698.

45 F. Birkhold, U. Meingast, P. Wassermann and O. Deutschmann, Modeling and simulation of the injection of urea-water-solution for automotive SCR DeNOx-systems, *Appl. Catal., B*, 2007, **70**(1–4), 119–127.

46 K. M. Thaler, L. Gilardi, M. Weber, A. Vohburger, Z. Toumasatos, A. Kontses, *et al.* HELIOS/SICRIT/mass spectrometry for analysis of aerosols in engine exhaust, *Aerosol Sci. Technol.*, 2021, **55**(8), 886–900.

47 J.-C. Wolf, M. Schaer, P. Siegenthaler and R. Zenobi, Direct quantification of chemical warfare agents and related compounds at low ppt levels: comparing active capillary dielectric barrier discharge plasma ionization and secondary electrospray ionization mass spectrometry, *Anal. Chem.*, 2015, **87**(1), 723–729.

48 F. Herrmann, B. Jochim, P. Oßwald, L. Cai, H. Pitsch and K. Kohse-Höinghaus, Experimental and numerical low-temperature oxidation study of ethanol and dimethyl ether, *Combust. Flame*, 2014, **161**(2), 384–397.

49 R. H. Boyd, Some physical properties of polyoxymethylene dimethyl ethers, *J. Polym. Sci.*, 1961, **50**(153), 133–141.

50 *Regulation No 49 of the Economic Commission for Europe of the United Nations (UN/ECE) – Uniform provisions concerning the measures to be taken against the emission of gaseous and particulate pollutants from compression-ignition engines and positive ignition engines for use in vehicles*; 2013.

51 L. Lautenschütz, D. Oestreich, P. Seidenspinner, U. Arnold, E. Dinjus and J. Sauer, Corrigendum to "Physico-chemical properties and fuel characteristics of oxymethylene dialkyl ethers" [Fuel 173 (2016) 129–137], *Fuel*, 2017, **209**, 812.

52 M. Elsener, D. Ferri, E. Jacob and O. Kröcher, Stability and reactivity of a polyoxymethylene dimethyl ether over typical catalysts of Diesel emission control: Manuscript in peer-review, *Top. Catal.*, 2022.

53 M. Etminan, G. Myhre, E. J. Highwood and K. P. Shine, Radiative forcing of carbon dioxide, methane, and nitrous oxide: A significant revision of the methane radiative forcing, *Geophys. Res. Lett.*, 2016, **43**(24), 12614–12623.

54 M. H. Fischer, The toxic effects of formaldehyde and formalin, *J. Exp. Med.*, 1905, **6**(4–6), 487–518.

55 R. J. G. Nuguid, M. Elsener, D. Ferri and O. Kröcher, Operando diffuse reflectance infrared detection of cyanide intermediate species during the reaction of formaldehyde with ammonia over $V_2O_5/WO_3\_TiO_2$, *Appl. Catal., B*, 2021, **298**, 120629.

56 N. Gaiser, T. Bierkandt, P. Oßwald, J. Zinsmeister, T. Kathrotia, S. Shaqiri, *et al.* Oxidation of oxymethylene ether (OME0−5): An experimental systematic study by mass spectrometry and photoelectron photoion coincidence spectroscopy, *Fuel*, 2021, 122650.

57 A. D. Gelner, D. Rothe, C. Kykal, M. Irwin, A. Sommer, C. Pastoetter, *et al.* Particle emissions of a heavy-duty engine fueled with polyoxymethylene dimethyl ethers (OME), *Environ. Sci.: Atmos.*, 2022, (2), 291–304.

58 C. Jin, X. Liu, T. Sun, J. D. Ampah, Z. Geng, J. Ji, *et al.* Preparation and performance improvement of methanol and palm oil/palm kernel oil blended fuel, *Fuel Process. Technol.*, 2021, **223**, 106996.